



NIH PUBLIC ACCESS

Author Manuscript

*Free Radic Biol Med.* Author manuscript; available in PMC 2015 August 01.

Published in final edited form as:

*Free Radic Biol Med.* 2014 August ; 73: 299–307. doi:10.1016/j.freeradbiomed.2014.06.001.

## Neuronal Uptake of Nanoformulated Superoxide Dismutase and Attenuation of Angiotensin II-Dependent Hypertension Following Central Administration

Krupa Savalia<sup>1</sup>, Devika S. Manickam<sup>2</sup>, Erin G. Rosenbaugh<sup>1</sup>, Jun Tian<sup>1</sup>, Iman M. Ahmad<sup>1,3</sup>, Alexander V. Kabanov<sup>2</sup>, and Matthew C. Zimmerman<sup>1,4</sup>

<sup>1</sup>Department of Cellular and Integrative Physiology, University of Nebraska Medical Center

<sup>2</sup>Division of Molecular Pharmaceutics and the Center for Nanomedicine in Drug Delivery, Eshelman School of Pharmacy, University of North Carolina, Chapel Hill, NC

<sup>3</sup>School of Allied Health Professionals, University of Nebraska Medical Center, Omaha, NE

<sup>4</sup>Center for Drug Delivery and Nanomedicine, University of Nebraska Medical Center, Omaha, NE

### Abstract

Excessive production of superoxide ( $O_2^{\bullet-}$ ) in the central nervous system has been widely implicated in the pathogenesis of cardiovascular diseases, including chronic heart failure and hypertension. In an attempt to overcome the failed therapeutic impact of currently available antioxidants in cardiovascular disease, we developed a nanomedicine-based delivery system for the  $O_2^{\bullet-}$  scavenging enzyme, copper/zinc superoxide dismutase (CuZnSOD), in which CuZnSOD protein is electrostatically bound to poly-L-lysine (PLL<sub>50</sub>)-polyethylene glycol (PEG) block copolymer to form CuZnSOD nanozyme. Different formulations of CuZnSOD nanozyme are covalently stabilized by either reducible or non-reducible crosslinked bonds between the PLL<sub>50</sub>-PEG polymers. Herein, we tested the hypothesis that PLL<sub>50</sub>-PEG CuZnSOD nanozyme delivers active CuZnSOD protein to neurons and decreases blood pressure in a mouse model of AngII-dependent hypertension. As determined by electron paramagnetic resonance (EPR) spectroscopy, nanozymes retain full SOD enzymatic activity as compared to native CuZnSOD protein. Non-reducible CuZnSOD nanozyme delivers active CuZnSOD protein to central neurons in culture (CATH.a neurons) without inducing significant neuronal toxicity. *In vivo* studies conducted in adult male C57BL/6 mice demonstrate that hypertension established by chronic subcutaneous infusion of AngII is significantly attenuated for up to 7 days following a single intracerebroventricular (ICV) injection of non-reducible nanozyme. These data indicate the efficacy of non-reducible PLL<sub>50</sub>-PEG CuZnSOD nanozyme in counteracting excessive  $O_2^{\bullet-}$  and decreasing blood pressure in AngII-dependent hypertensive mice following central administration.

© 2014 Elsevier Inc. All rights reserved.

Corresponding Author: Matthew C. Zimmerman, Ph.D., Associate Professor, Department of Cellular and Integrative Physiology, University of Nebraska Medical Center, Omaha, Nebraska 68198-5850, Phone: (402)559-7842, Fax: (402)559-4438, [mczimmerman@unmc.edu](mailto:mczimmerman@unmc.edu).

**Publisher's Disclaimer:** This is a PDF file of an unedited manuscript that has been accepted for publication. As a service to our customers we are providing this early version of the manuscript. The manuscript will undergo copyediting, typesetting, and review of the resulting proof before it is published in its final citable form. Please note that during the production process errors may be discovered which could affect the content, and all legal disclaimers that apply to the journal pertain.

Additionally, this study supports the further development of PLL<sub>50</sub>-PEG CuZnSOD nanozyme as an antioxidant-based therapeutic option for hypertension.

## Keywords

Hypertension; Angiotensin II; Superoxide; Superoxide Dismutase; Nanomedicine; Neurons

---

## INTRODUCTION

Excessive generation of reactive oxygen species (ROS), such as superoxide ( $O_2^{\bullet-}$ ), has been extensively implicated in several neurologically associated cardiovascular pathologies, including hypertension (1–5). As a major risk factor for myocardial infarction, stroke, heart failure, peripheral arterial disease, and chronic kidney disease, the morbidity and mortality associated with hypertension is a worldwide epidemic that is persistently rising (6). Although there are several standard therapies that effectively lower blood pressure in many patients, 34% of hypertensive patients in the United States who are under medical management (approximately 16 million people taking angiotensin converting enzyme inhibitors (ACEi), angiotensin receptor blockers (ARBs), diuretics, and beta-blockers) have uncontrolled blood pressure despite taking currently available prescription medications (7). Thus, there is a necessity to develop new pharmacotherapies that target novel molecular effectors (e.g.  $O_2^{\bullet-}$ ) that have been implicated by numerous studies to be integral in the pathogenesis of hypertension.

Angiotensin II (AngII), the primary effector peptide of the renin-angiotensin system, increases intracellular  $O_2^{\bullet-}$  levels by activating the angiotensin type 1 receptor (AT1R) on central neurons (3, 8). Our lab and others have previously shown that the AngII-induced increase in  $O_2^{\bullet-}$  contributes to the activation of neurons by modulating potassium ( $K^+$ ) and calcium ( $Ca^{2+}$ ) channel activity (5, 9, 10). Furthermore, AngII-induced activation of neurons in blood-brain barrier (BBB) deficient brain regions has been shown to increase sympathoexcitation, which contributes to hypertensive symptoms such as increased vasoconstriction, enhanced sodium and water reabsorption in the kidney, increased heart rate, and activation of T-lymphocytes and inflammatory cytokines (11–17).

One specific BBB-deficient region of particular importance in cardiovascular regulation is the subformal organ (SFO). The SFO lies at the roof of the third ventricle in the brain and is sensitive to circulating peptides and hormones, and to experimental treatments directly injected into the intracerebroventricular (ICV) system. Previous studies have demonstrated the successful scavenging of AngII-induced  $O_2^{\bullet-}$  with adenoviral-mediated overexpression of copper-zinc superoxide dismutase (CuZnSOD) in the SFO and other cardiovascular control brain regions, which in turn attenuates sympathetic drive and blood pressure in numerous hypertensive animal models (18–25). Although these studies convincingly demonstrate the beneficial anti-hypertensive effect of overexpressing CuZnSOD protein in the brain, clinical use of viral vectors in patients is limited by potential toxicity, overwhelming sequestration in the liver and aberrant inflammation (26–28).

In an attempt to overcome the failed therapeutic potential of viral-mediated gene transfer of CuZnSOD and antioxidant drug delivery, our group has developed chemically distinct nanoformulated complexes with CuZnSOD protein (nanozymes). We previously reported that intra-carotid injection of nanozyme complexes composed of polyethyleneimine (PEI)-polyethylene glycol (PEG) polymers, PEI-PEG, electrostatically bound to CuZnSOD protein, inhibits the central AngII-induced pressor response for three days (23). In an attempt to expand the therapeutic window of CuZnSOD nanozymes beyond three days, we generated a novel nanozyme formulation consisting of CuZnSOD protein complexed with cationic block copolymers, poly-L-lysine (PLL<sub>50</sub>)-polyethylene glycol (PEG) (29). We exploited the advantageous chemical properties of PLL<sub>50</sub>-PEG block copolymers and stabilized the complex by introducing reducible (disulfide bonds) or non-reducible (amide bonds) covalent bonds between the PLL<sub>50</sub> polymers using amine-reactive crosslinkers. Crosslinked nanozymes has been shown to significantly enhance delivery of nanoformulated complexes *in vitro* and *in vivo* (29–31).

Herein, we tested the hypothesis that crosslinked PLL<sub>50</sub>-PEG CuZnSOD nanozyme delivers functional CuZnSOD protein to neurons and attenuates blood pressure in chronically infused AngII-dependent hypertensive mice. We present data indicating that non-reducible crosslinked CuZnSOD nanozyme (cl-nanozyme) delivers active CuZnSOD protein to central neurons in culture without inducing significant toxicity, and is capable of attenuating elevated blood pressure in AngII-dependent hypertensive mice following ICV administration.

## MATERIALS AND METHODS

### Preparation of PLL<sub>50</sub>-PEG CuZnSOD Nanozyme

Synthesis, purification, and physicochemical characterization of PLL<sub>50</sub>-PEG CuZnSOD nanozymes were performed, as previously described (29). Briefly, native bovine CuZnSOD protein (Sigma-Aldrich, St. Louis, MO) was mixed with PLL<sub>50</sub>-PEG cationic block copolymer (Alamanda Polymers™, Huntsville, AL). To covalently stabilize the CuZnSOD nanozymes (Figure 1), reducible crosslinks were introduced using the commercially available chemical cross-linker, 3,3' dithiobis(sulfosuccinimidy-lproprionate) (DTSSP, Thermo Fisher Scientific, Rockford, IL); while non-reducible crosslinks were introduced using bis(sulfosuccinimidy)suberate (BS<sup>3</sup>, Thermo Fisher Scientific). The molar ratio of DTSSP/PLL<sub>50</sub> and BS<sup>3</sup>/PLL<sub>50</sub> were 0.5 and 1.0, respectively.

### Electron Paramagnetic Resonance (EPR) Spectroscopy

Enzymatic activity of PLL<sub>50</sub>-PEG CuZnSOD nanozymes was determined by measuring their ability to scavenge O<sub>2</sub><sup>•-</sup> in a cell-free system. EPR spectroscopy and the O<sub>2</sub><sup>•-</sup>-sensitive spin probe, 2,2,5,5-tetramethyl-pyrrolidine hydrochloride (CMH, 200 μmoles/L), were used to detect levels of O<sub>2</sub><sup>•-</sup> generated by hypoxanthine (HX, 25 μmoles/L) and xanthine oxidase (XO, 10 mU/mL in 100 μL of EPR buffer), as we previously described (23). Experimental samples included (each containing 400 U/mL of CuZnSOD protein): native CuZnSOD protein (Sigma-Aldrich), non-crosslinked nanozyme, reducible cl-nanozyme, or non-

reducible cl-nanozyme. EPR spectra were captured using a Bruker e-Scan Table-Top EPR spectrometer.

### **CATH.a Neuronal Cell Culture**

Mouse catecholaminergic CATH.a neurons were used as they have previously been identified as a reliable neuronal cell culture model for investigating AngII intra-neuronal signaling (32–34). CATH.a neurons (ATTC, stock no. CRL-11179) were cultured in RPMI-1640 medium, supplemented with 8% normal horse serum (NHS), 4% fetal bovine serum (FBS), and 1% penicillin-streptomycin, and maintained in a humidified incubator at 37°C with 5% CO<sub>2</sub>. Prior to experimentation, CATH.a neurons were differentiated for 6–8 days by adding N<sup>6</sup>,2'-O-dibutyryl adenosine 3',5'-cyclic monophosphate sodium salt (1mM, Sigma, St. Louis, MO, USA) to the culture medium every other day, as we previously described (5).

### **In Vitro Cytotoxicity Assay**

CATH.a neuronal toxicity was assessed using the Cell Counting Kit-8 (CCK-8, Dojindo Molecular Technologies, Inc.) according to the manufacturer's directions. Briefly, CATH.a neurons were incubated with CCK-8 solution (1:10 in serum-free media) for 1 hour prior to experimental treatment to obtain a baseline measurement of viable cells in culture. The number of live cells was indicated by the level of colored formazan product, as determined by measuring absorbance at 450nm. Following baseline assessment, the same CATH.a neuronal cultures were incubated with the following treatment groups (each containing 400 U/mL of CuZnSOD protein) for 1 and 3 hours to assess neuronal viability: native CuZnSOD protein, non-crosslinked nanozyme, reducible cl-nanozyme, non-reducible cl-nanozyme, or the equivalent amount of PLL<sub>50</sub>-PEG polymer alone. Twenty-four hours after removing treatment, percent cell viability was calculated by normalizing post-treatment formazan absorbance values to pre-treatment (i.e. baseline) absorbance values. The viability of vehicle-treated CATH.a neurons was considered as 100% survival.

### **Confocal Microscopy and Western Blot Analysis**

Neuronal uptake of CuZnSOD nanozyme was measured by labeling reducible cl-nanozyme and non-reducible cl-nanozyme with fluorescent rhodamine B isothiocyanate as we have previously described (23). Free rhodamine dye was removed from the labeled nanozyme sample by desalting the solution through an Illustra NAP-10 column (GE Healthcare). CATH.a neurons were treated for 1 or 3 hours with the rhodamine-labeled formulations and fluorescent images were captured with a Zeiss LSM 710 Meta Confocal Microscope.

To confirm neuronal delivery of nanozyme, we also performed Western blot analysis on cell lysates from differentiated CATH.a neurons exposed to the following treatment groups for 3 hours: vehicle, 400 U/mL native CuZnSOD protein, 400 U/mL non-crosslinked nanozyme, 400 U/mL reducible cl-nanozyme, or 400 U/mL non-reducible cl-nanozyme. Following treatment removal, neurons were rinsed with 1mL PBS and then incubated with 1mL Trypsin at 37°C and 5% CO<sub>2</sub> for 5 minutes to assist with removal of extracellular-bound proteins and nanozymes. CATH.a neurons were subsequently scraped on ice and centrifuged at 6,000 g for (4°C, 6 minutes). Pellet was rinsed with 100µL PBS to remove excess Trypsin

and centrifuged again at 6,000 g for (4°C, 6 minutes). Proteins were extracted using a lysis buffer (Complete Lysis-M, Roche Applied Science) and 25X protease inhibitor cocktail (P8340, Sigma Aldrich) and incubating the samples on ice for 15 minutes. Samples were subsequently sonicated and then centrifuged at 21,000 g (4°C, 10 minutes). After determining protein concentration, samples were mixed with the 15µl of 2X loading buffer and heated at 97°C for 15 minutes. Protein (30 µg) was separated by electrophoresis on a 12% sodium dodecyl sulfate (SDS)-polyacrylamide gel, and transferred to a nitrocellulose membrane. Membranes were probed with rabbit primary antibodies (Santa Cruz, CA) against CuZnSOD (1:500) and actin (1:1000).

### SOD Activity Assay

For determination of SOD activity levels, the same cell lysates as used for Western blot analysis were subjected to a total SOD Activity Kit-WST assay (Dojindo Molecular Technologies, Inc.) according to the manufacturer's directions.

### AngII Infused Mouse Model of Hypertension

Adult male C57Bl/6 mice aged 8–9 weeks (20–27 g; Harlan Laboratories, Indianapolis, IN) were housed in an animal facility with a 12-hour light-dark cycle and fed standard chow and water ad libitum. The following physiological parameters were measured daily in conscious mice using a radiotelemetry pressure transmitter device (Model TA11PA-C10, PhysioTel®, Data Sciences International): mean arterial pressure (MAP), heart rate (HR), systolic blood pressure (SBP), and diastolic blood pressure (DBP). Mice were anesthetized with isoflurane inhalation (0.5–2.0%) for subcutaneous implantation of the radiotelemetry device into the abdominal flank with the catheter inserted into the left carotid artery. Mice were also implanted with ICV cannulas under isoflurane anesthesia (–0.3mm dorsal, +1.0mm lateral to the bregma, and –3.0mm below the cerebral surface). Animals received topical bupivacaine on the procedure sites prior to closing the incision with suture. Following baseline blood pressure recordings for at least 3 days post-surgery, mice were subcutaneously implanted under isoflurane anesthesia with osmotic minipumps (Model 1002, Alzet®, DURECT Corporation) set to infuse AngII (400ng/kg/min, Sigma-Aldrich) over the period of several weeks. At day 9 of AngII infusion, when the mice were clearly hypertensive, a single bolus ICV injection of the following treatments groups was performed in conscious unrestrained mice: saline, PLL<sub>50</sub>-PEG shell, reducible cl-nanozyme or non-reducible cl-nanozyme (130–150 U CuZnSOD activity). Mice were euthanized with an overdose of pentobarbital (150mg/kg) administered by intraperitoneal injection. All procedures were performed in accordance with institutional guidelines for animal research reviewed and approved by the University of Nebraska Medical Center Institutional Animal Care and Use Committee.

### Statistical analysis

All data are expressed as mean ± SEM. For the EPR experiments, cytotoxicity and Western blot analysis, one-way ANOVA with Dunnett's post-hoc test was performed. For the SOD activity assay, Student's T-test with Welch's Correction was performed. For the *in vivo* experiments, we performed repeated measures two-way ANOVA with Dunnett's post-hoc test using time as a within-subject factor and treatment as a between-subject factor. *P*-value

less than 0.05 was considered statistically significant. Statistical analyses were performed using Prism (GraphPad Software, Inc.) or Statistical Package for Social Sciences software (SPSS, Inc.).

## RESULTS

### CuZnSOD Nanozymes Scavenge Superoxide

To examine activity of CuZnSOD nanozymes, we tested their ability to scavenge  $O_2^{\bullet-}$  in a cell-free system using EPR spectroscopy. The reducible cl-nanozyme and non-reducible cl-nanozyme were as effective as native CuZnSOD protein in decreasing the EPR spectra (Figure 2A). Summary data (Figure 2B) clearly reveal a significant decrease in EPR spectra amplitude in all samples containing CuZnSOD as compared to vehicle. These data clearly validate the  $O_2^{\bullet-}$  scavenging capacity of our PLL<sub>50</sub>-PEG CuZnSOD nanozyme formulations, and confirm that the nanozyme structure does not preclude access to the substrate nor does the protein need to be released for it to catalyze  $O_2^{\bullet-}$  dismutation, as previously reported (35, 36).

### Non-Reducible Crosslinked Nanozyme is the Least Toxic Formulation *in vitro*

We next determined the potential neuronal toxicity induced by nanozyme treatment *in vitro*. CATH.a neurons were treated for 1 or 3 hours with vehicle, native CuZnSOD protein, PLL<sub>50</sub>-PEG shell alone, non-crosslinked nanozyme, reducible cl-nanozyme, or non-reducible cl-nanozyme, and 24 hours later cell survival was determined. Summary data (Figure 3) reveal no significant difference in survival between neurons treated with native CuZnSOD protein and vehicle. However, PLL<sub>50</sub>-PEG shell alone, non-crosslinked nanozyme, and reducible cl-nanozyme did induce significant toxicity. In contrast, the non-reducible cl-nanozyme did not induce neuronal cell death following 1 hour treatment. However, there was a modest decline in cell survival following 3 hour treatment with non-reducible cl-nanozyme. These data identify non-reducible cl-CuZnSOD nanozyme as the safest formulation tested in cultured neurons.

### Crosslinked Nanozymes Enhance Neuronal Uptake of CuZnSOD Protein

To evaluate the ability of cl-nanozymes to be taken up by neurons in culture, CATH.a neurons were exposed to fluorescent rhodamine-labeled CuZnSOD nanozymes for either 1 or 3 hours. Representative confocal microscopy images (Figure 4) of CATH.a neurons exposed to cl-nanozymes reveal uptake of either reducible cl-nanozyme or non-reducible cl-nanozyme as early as 1 hour after exposure, with even greater uptake after 3 hours as indicated by increased red fluorescence.

### Non-Reducible Crosslinked Nanozymes Delivers Active CuZnSOD Protein to Neurons

To confirm uptake of nanozymes *in vitro*, Western blot analysis was performed on lysates from CATH.a neurons treated for 3 hours with vehicle, native CuZnSOD protein, non-crosslinked nanozyme, reducible cl-nanozyme, or non-reducible cl-nanozyme. The representative Western blot and summary data (Figure 5A) show a significant increase in CuZnSOD protein levels in neurons treated with non-reducible cl-nanozyme. It should be noted that the bovine CuZnSOD protein, which is used in our nanozymes, migrates slower

in gel electrophoresis. Next, we examined the activity of nanozyme-delivered CuZnSOD protein. SOD activity in CATH.a neurons treated with native CuZnSOD protein, non-crosslinked nanozyme, and reducible cl-nanozyme was slightly elevated when compared to vehicle-treated neurons, although these differences were not statistically significant (Figure 5B). However, SOD activity was significantly elevated in neurons treated with non-reducible cl-nanozyme. Collectively, the confocal microscopy images (Figure 4), Western blot analysis (Figure 5A), and SOD activity assay (Figure 5B) clearly identify the non-reducible cl-nanozyme as the most effective formulation in delivering active CuZnSOD protein to neurons in culture.

### **ICV-administered Non-Reducible Crosslinked CuZnSOD Nanozyme Significantly Attenuates AngII-dependent Hypertension**

We next evaluated the anti-hypertensive therapeutic potential of our cl-nanozymes in an AngII-infused hypertensive mouse model. Mean arterial pressure (MAP) was recorded from mice subcutaneously infused with AngII (400ng/kg/min) before and after a single ICV injection of saline, PLL<sub>50</sub>-PEG shell alone, reducible cl-nanozyme or non-reducible cl-nanozyme. An immediate (i.e. within 24 hours) increase in blood pressure following implantation of AngII-filled osmotic minipumps was observed in all groups, with an average increase of 24 mmHg on day 1 of AngII infusion (Figure 6A). There were no significant differences in the degree of elevation in MAP between the various groups of mice at day 1 of AngII infusion ( $p > 0.05$ ). Mice were ICV injected with the treatments listed above at day 9 of AngII infusion as this was the time point at which the blood pressures stabilized in the hypertensive range (average MAP = 131 mmHg; average change from baseline (day 0) MAP = 42 mmHg;  $p < 0.05$  versus baseline MAP in each respective group). Importantly, the hypertensive MAPs at day 9 were similar between all groups with no significant differences observed ( $p > 0.05$ ): Saline  $128 \pm 3$  mmHg, PLL<sub>50</sub>-PEG shell  $123 \pm 3$  mmHg, Reducible cl-nanozyme  $138 \pm 5$  mmHg, Non-reducible cl-nanozyme  $133 \pm 5$  mmHg.

After a single ICV injection of saline, PLL<sub>50</sub>-PEG shell, or reducible cl-nanozyme at day 9 of AngII infusion, mice continued to remain hypertensive for the duration of AngII infusion (Figure 6A). In contrast, ICV injection of non-reducible cl-nanozyme significantly decreased MAP and DBP within 24 hours and for up to 7 days (Figure 6A, D). There was also a decrease, although not statistically significant ( $p=0.085$ ), in SBP in mice ICV injected with non-reducible cl-nanozyme (Figure 6C). ICV injection of saline, PLL<sub>50</sub>-PEG shell, reducible cl-nanozyme, or non-reducible cl-nanozyme did not alter heart rate (Figure 6B). It should be noted that MAP, SBP, and DBP in all groups returned to near baseline (c.a. Day 20–21 of AngII infusion) after the AngII-filled osmotic minipumps emptied. These *in vivo* data indicate that the non-reducible cl-nanozyme attenuates AngII-dependent hypertension following ICV administration.

## **DISCUSSION**

Our present study demonstrates the utility of PLL<sub>50</sub>-PEG nanoformulated CuZnSOD protein as a potentially viable pharmacotherapy for AngII-dependent neurogenic hypertension. The data presented in this study reveal that CuZnSOD cl-nanozymes retain enzymatic activity

and are able to effectively scavenge  $O_2^{\bullet-}$ . Furthermore, the non-reducible cl-nanozyme delivers active CuZnSOD protein to central neurons in culture more efficiently than native CuZnSOD protein, non-crosslinked nanozyme, or the reducible cl-nanozyme. Lastly, our *in vivo* experiments demonstrate the therapeutic potential of the non-reducible cl-nanozyme formulation and its ability to significantly attenuate hypertensive blood pressure for up to 7 days following a single ICV injection in AngII-hypertensive mice. Taken together, our data strongly support the further development of non-reducible cl-nanozymes for the improved treatment of hypertension in which there are excessive levels of  $O_2^{\bullet-}$  in the central nervous system.

Previous studies by numerous groups have clearly demonstrated that increased scavenging of  $O_2^{\bullet-}$  in the brain, via adenoviral-mediated overexpression of CuZnSOD or SOD mimetics, decreases blood pressure and attenuates sympathoexcitation in various animal models of hypertension (18–25). For example, adenovirus-mediated overexpression of CuZnSOD in the SFO or rostral ventrolateral medulla (RVLM) of the brain decreases blood pressure in AngII-infused hypertensive mice and spontaneously hypertensive rats (SHR), respectively (18, 19). In addition, CuZnSOD overexpression in the RVLM decreases blood pressure and reduces sympathetic vasomotor tone in the 2 kidney-1 clip hypertensive rat model (37). Central administration of tempol, an SOD mimetic, attenuates the increase in blood pressure and renal sympathetic nerve activity induced by ICV infusion of AngII (38). Although these previous studies and others have convincingly demonstrated a beneficial anti-hypertensive effect of overexpressing  $O_2^{\bullet-}$  scavengers in the brain, the use of viral vectors or SOD mimetics in clinical practice is limited by poor cellular uptake, rapid clearance, toxicity, end-organ sequestration, and/or inflammation (26–28). Furthermore, it is essential to develop clinically acceptable therapeutic strategies with relevant routes of drug delivery (i.e. intravenous, intranasal, or sublingual administration). Thus, it becomes increasingly important to investigate new therapeutic strategies which may address these pharmacokinetic obstacles in drug delivery and development.

Collectively, the extensive evidence establishing the benefit of scavenging  $O_2^{\bullet-}$  in the brain provides rationale for our experiments in which we investigate the efficacy of a therapeutically relevant antioxidant strategy for the improved treatment of hypertension. One promising drug delivery option includes implementation of nanotechnology. The utilization of nanoparticles has been shown to improve solubility and long term stability of pharmacological agents through prevention of premature clearance by the renal or reticulo-endothelial systems (39). As such, we believe there is great utility in developing nanoformulated CuZnSOD protein as an antioxidant therapeutic strategy for hypertension. We previously reported that a non-crosslinked formulation of CuZnSOD nanozyme, in which the block copolymer PEI-PEG is electrostatically bound to CuZnSOD protein, inhibits the acute central AngII-induced pressor response for three days (23). These initial experiments prompted us to explore other chemically distinct nanoformulations, in which complexes are stabilized with reducible or non-reducible crosslinked bonds between the PLL<sub>50</sub>-PEG block copolymers, with the intention of expanding the therapeutic window. Using these crosslinked complexes and a more relevant model of hypertension (i.e. chronic subcutaneous infusion of AngII) in the current study, our data presented herein clearly



demonstrate the  $O_2^{\bullet-}$  scavenging capacity of crosslinked nanozymes and identify the non-reducible cl-nanozyme as the ideal nanoformulation to safely deliver active CuZnSOD protein to neurons in culture. Furthermore, the non-reducible CuZnSOD cl-nanozyme significantly decreased MAP and DBP in AngII hypertensive mice following ICV administration. In addition, SBP was decreased, although not statistically significant ( $P=0.085$ ), in mice ICV injected with the non-reducible cl-nanozyme. Collectively, these data suggest that ICV-administered non-reducible cl-nanozyme decreases blood pressure in AngII-dependent hypertensive mice by influencing both preload and afterload, and inhibiting sympathetic output. Future studies in which the non-reducible cl-nanozyme is peripherally administered (i.e. intravenously, intranasally, or sublingually) are needed to determine the direct effect, if any, of the nanozyme on cardiac function.

The integral involvement of  $O_2^{\bullet-}$  in the pathogenesis of hypertension has been implicated and recapitulated in numerous animal models over the years. As a downstream signaling molecule in the renin-angiotensin-aldosterone system (RAAS) pathway, there is also mounting evidence that excessive levels of  $O_2^{\bullet-}$  in hypertension are generated by immunological changes (i.e. activation of T cells and cytokines) (14, 15, 40-42). As such, we posit our  $O_2^{\bullet-}$  scavenging CuZnSOD nanozymes may have an added benefit over traditionally prescribed pharmacotherapies for hypertension, which specifically target the RAAS pathway (ACE inhibitors; ARBs), as they will scavenge  $O_2^{\bullet-}$  produced from multiple stimuli (i.e. AngII and cytokines). In fact, it has been reported that increased  $O_2^{\bullet-}$  scavenging in hypertensive rats via peripheral administration of tempol prevents vascular dysfunction and improves renal blood perfusion to a greater extent than the ARB candesartan (43, 44). To this extent, future studies will not only compare our peripherally administered CuZnSOD nanozymes with standard antihypertensive medications, but will also examine synergistic or additive therapeutic efficacy of CuZnSOD nanozyme given in combination with standard antihypertensive drugs.

While the results from our current study are promising, there are several considerations which must be addressed in further developing this nanoformulated therapeutic strategy for human hypertensive patients resistant to currently available pharmacotherapy. Considering previous studies have shown that increased  $O_2^{\bullet-}$  scavenging in neurons inhibits the AngII-induced modulation of ion channel activity and increases neuronal firing (23, 45), we speculate that neurons in cardiovascular control brain regions surrounding the ventricular system, such as the SFO, internalize the non-reducible cl-nanozyme following ICV injection. However, since our nanozymes are not designed to specifically target neurons, it is plausible that other cell types in the brain also internalize the complexes. It is certainly feasible to further develop nanoparticles to target cell-specific populations, as Muzykantov and colleagues have successfully performed with other CuZnSOD nanoformulations targeted to endothelial cells (46–50). Nonetheless, supplementary studies are needed to determine the cellular distribution of non-reducible cl-nanozyme following *in vivo* administration.

In addition, the precise subcellular localization of the cl-nanozymes following neuronal uptake remains unclear. However, there seems to be a clear distinction in the cellular distribution of reducible cl-nanozyme versus non-reducible cl-nanozyme, as indicated by the

representative confocal microscopy images (Figure 4). The reducible formulation shows punctate staining throughout the cell, while the non-reducible formulation shows both punctate staining in the cell as well as distribution along the plasma membrane. We believe this differential distribution is a reflection of the distinct chemical properties of the two crosslinked formulations. The reducible cl-nanozyme is composed of disulfide bonds which may easily disassociate in the intracellular reducing environment. While the non-reducible cl-nanozyme is composed of more stable amide bonds and is thus likely to remain intact in the intracellular environment. We posit that the non-reducible cl-nanozyme associated with the plasma membrane may be of therapeutic benefit as it could easily scavenge  $O_2^{\bullet-}$  generated from membrane-bound NADPH oxidase, one of the primary sources of AngII-induced  $O_2^{\bullet-}$  production in neurons (2). This theory may indeed identify the mechanism whereby non-reducible cl-nanozyme achieves therapeutic efficacy following ICV injection *in vivo* (Figure 6A). However, additional studies are needed to address this hypothesis. An additional explanation as to why the reducible cl-nanozyme had no effect on the elevated MAP in the AngII-infused mice is that the disulfide bonds between the polymers are reduced upon injection into the brain, which allows for the polymer to dissociate from the protein, resulting in the release of CuZnSOD protein from the complex. It is well-accepted that free CuZnSOD protein does not permeate cell membranes and thus the reducible cl-nanozyme may fail to deliver active CuZnSOD protein to neurons *in vivo*. These theories identify potential mechanisms whereby non-reducible cl-nanozyme, but not reducible cl-nanozyme, achieves therapeutic efficacy following ICV injection.

It is important to highlight that our cell culture experiments were performed using the catecholaminergic CATH.a neuronal cell line. Although these neurons have been widely identified in the literature as exhibiting similar AngII intra-neuronal signaling mechanisms as primary neurons isolated from the hypothalamus and brainstem (33), future experiments must include the utilization of primary neurons cultured from the brains of AngII-infused hypertensive mice. Additionally, we must consider that the potential toxicity of the cl-nanozymes *in vitro* may not necessarily duplicate the noxious or immunogenic mechanisms which occur in a full-body *in vivo* animal model. In regards to our *in vitro* toxicity study (Figure 3), the PLL<sub>50</sub>-PEG shell causes a marked decrease in neuronal cell survival most likely because the highly positively charged PLL polymers damage the cells via interaction with the negatively charged cell membrane and other macromolecules. This toxicity induced by positively charged polymers is well-documented (51, 52). It should also be noted that we posit that the non-crosslinked CuZnSOD nanozyme is as toxic as the PLL<sub>50</sub>-PEG shell alone because the polymer shell dissociates from the enzyme (as it is not crosslinked) allowing for free positively charged PLL<sub>50</sub>-PEG to damage the cells. Furthermore, we speculate that upon entering the reducing intracellular environment, the reducible disulfide bonds between the PLL polymers of the reducible cl-nanozyme are cleaved and consequently release the positively charged and cytotoxic PLL<sub>50</sub>-PEG shell resulting in mild, yet significant neuronal toxicity (Figure 3). These toxicity data may provide some explanation for the discrepancy between the CuZnSOD protein and activity levels detected in the non-crosslinked nanozyme group (Figure 5). It should be noted that the SOD activity assay we used does not specifically measure CuZnSOD activity; rather, it measures total SOD activity (including manganese SOD and extracellular SOD). Cells treated with non-crosslinked nanozyme did

not show an increase in CuZnSOD protein, but did show an increase, although not statistically significant compared to vehicle-treated cells, in SOD activity. We posit that the increase in SOD activity observed in the non-crosslinked nanozyme treated cells is due to increased activity of the other SOD isozymes. We believe the other SOD isozymes, particularly MnSOD, may become more active in these cells in attempt to combat the toxicity induced by the non-crosslinked nanozyme formulation, as shown in Figure 3. However, additional experiments are needed to test this hypothesis. Collectively, these data further support the benefit, in terms of potential cellular toxicity, for chemically crosslinking the PLL<sub>50</sub>-PEG shell with non-reducible covalent bonds. Nonetheless, it will be imperative to investigate the potential cellular toxicity in multiple cell populations (e.g. endothelial cells, astroglia, microglia, oligodendrocytes, etc.) and following more clinically relevant routes of cl-nanozyme administration *in vivo*.

In conclusion, the experimental data presented in this paper provide sufficient evidence supporting the delivery of active CuZnSOD protein to neurons by nanomedicine-based technologies for the treatment of AngII-dependent hypertension. This distinct crosslinked nanoformulated drug delivery system provides an alternative strategy for targeting specific downstream signaling molecules in the RAAS pathway, namely O<sub>2</sub><sup>•-</sup>, known to play a critical role in the pathogenesis of hypertension. The promising results from our *in vitro* experiments, coupled with the therapeutic efficacy as illustrated by the attenuated blood pressures in AngII-infused hypertensive mice following central administration with non-reducible cl-nanozyme, warrants further investigation to pursue these novel nanoformulations as a therapeutic option for the improved treatment of hypertension.

## Acknowledgments

### FUNDING

This work was supported by a project on the National Institute of General Medical Sciences Center of Biomedical Research Excellence (COBRE) grant [P20GM103480, formerly P20RR02193 to MCZ] and a University of Nebraska Medical Center Graduate Student Assistantship (KS). MCZ is also supported by the National Heart, Lung, and Blood Institute at the National Institutes of Health [R01HL103942].

We acknowledge the assistance of the Nanomaterials Core facility of the Center for Biomedical Research Excellence (CoBRE): Nebraska Center for Nanomedicine supported by the Institutional Development Award (IDeA) from the National Institute of General Medical Sciences of the National Institutes of Health [P20GM103480]. We also thank Janice A. Taylor and James R. Talaska of the Confocal Laser Scanning Microscope Core Facility at the University of Nebraska Medical Center for providing assistance with confocal microscopy and the Nebraska Research Initiative and the Eppley Cancer Center for their support of the Core Facility. Additionally, AVK and DSM gratefully acknowledge the support of *The Carolina Partnership*, a strategic partnership between the UNC Eshelman School of Pharmacy and The University Cancer Research Fund through the Lineberger Comprehensive Cancer Center.

## References

1. Chan SH, Hsu KS, Huang CC, Wang LL, Ou CC, Chan JY. NADPH oxidase-derived superoxide anion mediates angiotensin II-induced pressor effect via activation of p38 mitogen-activated protein kinase in the rostral ventrolateral medulla. *Circ Res.* 2005 Oct 14; 97(8):772–780. [PubMed: 16151022]
2. Zimmerman MC, Dunlay RP, Lazartigues E, Zhang Y, Sharma RV, Engelhardt JF, Davisson RL. Requirement for Rac1-dependent NADPH oxidase in the cardiovascular and dipsogenic actions of angiotensin II in the brain. *Circ Res.* 2004 Sep 3; 95(5):532–539. [PubMed: 15271858]

3. Zimmerman MC, Davisson RL. Redox signaling in central neural regulation of cardiovascular function. *Prog Biophys Mol Biol.* 2004 Feb-Apr;84(2-3):125-149. [PubMed: 14769433]
4. Nozoe M, Hirooka Y, Koga Y, Araki S, Konno S, Kishi T, Ide T, Sunagawa K. Mitochondria-derived reactive oxygen species mediate sympathoexcitation induced by angiotensin II in the rostral ventrolateral medulla. *J Hypertens.* 2008 Nov; 26(11):2176-2184. [PubMed: 18854758]
5. Yin JX, Yang RF, Li S, Renshaw AO, Li YL, Schultz HD, Zimmerman MC. Mitochondria-produced superoxide mediates angiotensin II-induced inhibition of neuronal potassium current. *Am J Physiol Cell Physiol.* 2010 Apr; 298(4):C857-65. [PubMed: 20089930]
6. Roger VL, Go AS, Lloyd-Jones DM. Heart disease and stroke statistics--2012 update: A report from the american heart association. *Circulation.* 2012 Jan 3; 125(1):e2-e220. [PubMed: 22179539]
7. Valderrama AL, Gillespie C, Coleman King S, George MG, Hong Y. Vital signs: Awareness and treatment of uncontrolled hypertension among adults - united states, 2003-2010. *Morbidity and Mortality Weekly Report, MMWR.* 2012 Sep 4; 61(35):703-709.
8. Simpson JB. The circumventricular organs and the central actions of angiotensin. *Neuroendocrinology.* 1981 Apr; 32(4):248-256. [PubMed: 7012657]
9. Zimmerman MC, Sharma RV, Davisson RL. Superoxide mediates angiotensin II-induced influx of extracellular calcium in neural cells. *Hypertension.* 2005 Apr; 45(4):717-723. [PubMed: 15699459]
10. Summers C, Zhu M, Gelband CH, Posner P. Angiotensin II type 1 receptor modulation of neuronal K<sup>+</sup> and Ca<sup>2+</sup> currents: Intracellular mechanisms. *Am J Physiol.* 1996 Jul; 271(1 Pt 1):C154-63. [PubMed: 8760041]
11. San Martin A, Griendling KK. Redox control of vascular smooth muscle migration. *Antioxid Redox Signal.* 2010 Mar 1; 12(5):625-640. [PubMed: 19737088]
12. Touyz RM. Reactive oxygen species and angiotensin II signaling in vascular cells -- implications in cardiovascular disease. *Braz J Med Biol Res.* 2004 Aug; 37(8):1263-1273. [PubMed: 15273829]
13. Touyz RM, Tabet F, Schiffrin EL. Redox-dependent signalling by angiotensin II and vascular remodelling in hypertension. *Clin Exp Pharmacol Physiol.* 2003 Nov; 30(11):860-866. [PubMed: 14678251]
14. Marvar PJ, Thabet SR, Guzik TJ, Lob HE, McCann LA, Weyand C, Gordon FJ, Harrison DG. Central and peripheral mechanisms of T-lymphocyte activation and vascular inflammation produced by angiotensin II-induced hypertension. *Circ Res.* 2010 Jul 23; 107(2):263-270. [PubMed: 20558826]
15. Harrison DG, Marvar PJ, Titze JM. Vascular inflammatory cells in hypertension. *Front Physiol.* 2012; 3:128. [PubMed: 22586409]
16. Lassegue B, Griendling KK. NADPH oxidases: Functions and pathologies in the vasculature. *Arterioscler Thromb Vasc Biol.* 2010 Apr; 30(4):653-661. [PubMed: 19910640]
17. Touyz RM. Oxidative stress and vascular damage in hypertension. *Curr Hypertens Rep.* 2000 Feb; 2(1):98-105. [PubMed: 10981135]
18. Chan SH, Tai MH, Li CY, Chan JY. Reduction in molecular synthesis or enzyme activity of superoxide dismutases and catalase contributes to oxidative stress and neurogenic hypertension in spontaneously hypertensive rats. *Free Radic Biol Med.* 2006 Jun 1; 40(11):2028-2039. [PubMed: 16716903]
19. Zimmerman MC, Lazartigues E, Sharma RV, Davisson RL. Hypertension caused by angiotensin II infusion involves increased superoxide production in the central nervous system. *Circ Res.* 2004 Jul 23; 95(2):210-216. [PubMed: 15192025]
20. Lindley TE, Doobay MF, Sharma RV, Davisson RL. Superoxide is involved in the central nervous system activation and sympathoexcitation of myocardial infarction-induced heart failure. *Circ Res.* 2004 Feb 20; 94(3):402-409. [PubMed: 14684626]
21. Yin M, Wheeler MD, Connor HD, Zhong Z, Bunzendahl H, Dikalova A, Samulski RJ, Schoonhoven R, Mason RP, Swenberg JA, Thurman RG. Cu/zn-superoxide dismutase gene attenuates ischemia-reperfusion injury in the rat kidney. *J Am Soc Nephrol.* 2001 Dec; 12(12):2691-2700. [PubMed: 11729238]

22. Zimmerman MC, Lazartigues E, Lang JA, Sinnayah P, Ahmad IM, Spitz DR, Davisson RL. Superoxide mediates the actions of angiotensin II in the central nervous system. *Circ Res*. 2002 Nov 29; 91(11):1038–1045. [PubMed: 12456490]
23. Rosenbaugh EG, Roat JW, Gao L, Yang RF, Manickam DS, Yin JX, Schultz HD, Bronich TK, Batrakova EV, Kabanov AV, Zucker IH, Zimmerman MC. The attenuation of central angiotensin II-dependent pressor response and intra-neuronal signaling by intracarotid injection of nanoformulated copper/zinc superoxide dismutase. *Biomaterials*. 2010 Jul; 31(19):5218–5226. [PubMed: 20378166]
24. Ding Y, Li YL, Zimmerman MC, Davisson RL, Schultz HD. Role of CuZn superoxide dismutase on carotid body function in heart failure rabbits. *Cardiovasc Res*. 2009 Mar 1; 81(4):678–685. [PubMed: 19091790]
25. Woo YJ, Zhang JC, Vijayasathy C, Zwacka RM, Englehardt JF, Gardner TJ, Sweeney HL. Recombinant adenovirus-mediated cardiac gene transfer of superoxide dismutase and catalase attenuates postischemic contractile dysfunction. *Circulation*. 1998 Nov 10; 98(19 Suppl):II255–60. discussion II260–1. [PubMed: 9852911]
26. Costantini LC, Bakowska JC, Breakefield XO, Isacson O. Gene therapy in the CNS. *Gene Ther*. 2000 Jan; 7(2):93–109. [PubMed: 10673714]
27. Alemany R, Suzuki K, Curiel DT. Blood clearance rates of adenovirus type 5 in mice. *J Gen Virol*. 2000 Nov; 81(Pt 11):2605–2609. [PubMed: 11038370]
28. Descamps D, Benihoud K. Two key challenges for effective adenovirus-mediated liver gene therapy: Innate immune responses and hepatocyte-specific transduction. *Curr Gene Ther*. 2009 Apr; 9(2):115–127. [PubMed: 19355869]
29. Manickam DS, Brynskikh AM, Kopanic JL, Sorgen PL, Klyachko NL, Batrakova EV, Bronich TK, Kabanov AV. Well-defined cross-linked antioxidant nanozymes for treatment of ischemic brain injury. *J Control Release*. 2012 Sep 28; 162(3):636–645. [PubMed: 22902590]
30. Klyachko NL, Haney MJ, Zhao Y, Manickam DS, Mahajan V, Suresh P, Hingtgen SD, Mosley RL, Gendelman HE, Kabanov AV, Batrakova EV. Macrophages offer a paradigm switch for CNS delivery of therapeutic proteins. *Nanomedicine (Lond)*. 2013 Nov 18.
31. Klyachko NL, Manickam DS, Brynskikh AM, Uglanova SV, Li S, Higginbotham SM, Bronich TK, Batrakova EV, Kabanov AV. Cross-linked antioxidant nanozymes for improved delivery to CNS. *Nanomedicine*. 2012 Jan; 8(1):119–129. [PubMed: 21703990]
32. Sun C, Sumners C, Raizada MK. Chronotropic action of angiotensin II in neurons via protein kinase C and CaMKII. *Hypertension*. 2002 Feb; 39(2 Pt 2):562–566. [PubMed: 11882608]
33. Sun C, Du J, Raizada MK, Sumners C. Modulation of delayed rectifier potassium current by angiotensin II in CATH.a cells. *Biochem Biophys Res Commun*. 2003 Oct 24; 310(3):710–714. [PubMed: 14550259]
34. Zhu M, Gelband CH, Posner P, Sumners C. Angiotensin II decreases neuronal delayed rectifier potassium current: Role of calcium/calmodulin-dependent protein kinase II. *J Neurophysiol*. 1999 Sep; 82(3):1560–1568. [PubMed: 10482769]
35. Klyachko NL, Manickam DS, Brynskikh AM, Uglanova SV, Li S, Higginbotham SM, Bronich TK, Batrakova EV, Kabanov AV. Cross-linked antioxidant nanozymes for improved delivery to CNS. *Nanomedicine*. 2012 Jan; 8(1):119–129. [PubMed: 21703990]
36. Manickam DS, Brynskikh AM, Kopanic JL, Sorgen PL, Klyachko NL, Batrakova EV, Bronich TK, Kabanov AV. Well-defined cross-linked antioxidant nanozymes for treatment of ischemic brain injury. *J Control Release*. 2012 Sep 28; 162(3):636–645. [PubMed: 22902590]
37. Oliveira-Sales EB, Colombari DS, Davisson RL, Kasparov S, Hirata AE, Campos RR, Paton JF. Kidney-induced hypertension depends on superoxide signaling in the rostral ventrolateral medulla. *Hypertension*. 2010 Aug; 56(2):290–296. [PubMed: 20606111]
38. Campese VM, Shaohua Y, Huiquin Z. Oxidative stress mediates angiotensin II-dependent stimulation of sympathetic nerve activity. *Hypertension*. 2005 Sep; 46(3):533–539. [PubMed: 16116043]
39. Rosenbaugh EG, Savalia KK, Manickam DS, Zimmerman MC. Antioxidant-based therapies for angiotensin II-associated cardiovascular diseases. *Am J Physiol Regul Integr Comp Physiol*. 2013 Jun 1; 304(11):R917–28. [PubMed: 23552499]

40. Harrison DG, Guzik TJ, Lob HE, Madhur MS, Marvar PJ, Thabet SR, Vinh A, Weyand CM. Inflammation, immunity, and hypertension. *Hypertension*. 2011 Feb; 57(2):132–140. [PubMed: 21149826]
41. Marvar PJ, Lob H, Vinh A, Zarreen F, Harrison DG. The central nervous system and inflammation in hypertension. *Curr Opin Pharmacol*. 2011 Apr; 11(2):156–161. [PubMed: 21196131]
42. Lob HE, Marvar PJ, Guzik TJ, Sharma S, McCann LA, Weyand C, Gordon FJ, Harrison DG. Induction of hypertension and peripheral inflammation by reduction of extracellular superoxide dismutase in the central nervous system. *Hypertension*. 2010 Feb; 55(2):277–83. 6. p following 283. [PubMed: 20008675]
43. Costa CA, Amaral TA, Carvalho LC, Ognibene DT, da Silva AF, Moss MB, Valenca SS, de Moura RS, Resende AC. Antioxidant treatment with tempol and apocynin prevents endothelial dysfunction and development of renovascular hypertension. *Am J Hypertens*. 2009 Dec; 22(12):1242–1249. [PubMed: 19779472]
44. Palm F, Onozato M, Welch WJ, Wilcox CS. Blood pressure, blood flow, and oxygenation in the clipped kidney of chronic 2-kidney, 1-clip rats: Effects of tempol and angiotensin blockade. *Hypertension*. 2010 Feb; 55(2):298–304. [PubMed: 20048199]
45. Sun C, Sellers KW, Sumners C, Raizada MK. NAD(P)H oxidase inhibition attenuates neuronal chronotropic actions of angiotensin II. *Circ Res*. 2005 Apr 1; 96(6):659–666. [PubMed: 15746442]
46. Shuvaev VV, Han J, Tliba S, Arguiri E, Christofidou-Solomidou M, Ramirez SH, Dykstra H, Persidsky Y, Atochin DN, Huang PL, Muzykantov VR. Anti-inflammatory effect of targeted delivery of SOD to endothelium: Mechanism, synergism with NO donors and protective effects in vitro and in vivo. *PLoS One*. 2013 Oct 11.8(10):e77002. [PubMed: 24146950]
47. Hood ED, Greineder CF, Dodia C, Han J, Mesaros C, Shuvaev VV, Blair IA, Fisher AB, Muzykantov VR. Antioxidant protection by PECAM-targeted delivery of a novel NADPH-oxidase inhibitor to the endothelium in vitro and in vivo. *J Control Release*. 2012 Oct 28; 163(2):161–169. [PubMed: 22974832]
48. Howard MD, Greineder CF, Hood ED, Muzykantov VR. Endothelial targeting of liposomes encapsulating SOD/catalase mimetic EUK-134 alleviates acute pulmonary inflammation. *J Control Release*. 2014 Jan 9.177C:34–41. [PubMed: 24412573]
49. Hood ED, Chorny M, Greineder CF, Alferiev SI, Levy RJ, Muzykantov VR. Endothelial targeting of nanocarriers loaded with antioxidant enzymes for protection against vascular oxidative stress and inflammation. *Biomaterials*. 2014 Jan 27.
50. Muzykantov VR. Targeting of superoxide dismutase and catalase to vascular endothelium. *J Control Release*. 2001 Mar 12; 71(1):1–21. [PubMed: 11245904]
51. Godbey WT, Wu KK, Mikos AG. Poly(ethylenimine)-mediated gene delivery affects endothelial cell function and viability. *Biomaterials*. 2001 Mar; 22(5):471–480. [PubMed: 11214758]
52. Moghimi SM, Symonds P, Murray JC, Hunter AC, Debska G, Szewczyk A. A two-stage poly(ethylenimine)-mediated cytotoxicity: Implications for gene transfer/therapy. *Mol Ther*. 2005 Jun; 11(6):990–995. [PubMed: 15922971]

**HIGHLIGHTS**

- PLL<sub>50</sub>-PEG CuZnSOD nanozymes effectively scavenge superoxide
- Non-reducible crosslinked nanozymes deliver active CuZnSOD protein to neurons
- Non-reducible crosslinked CuZnSOD nanozyme attenuates AngII hypertension
- Nanomedicine is a therapeutically relevant drug delivery strategy for antioxidants

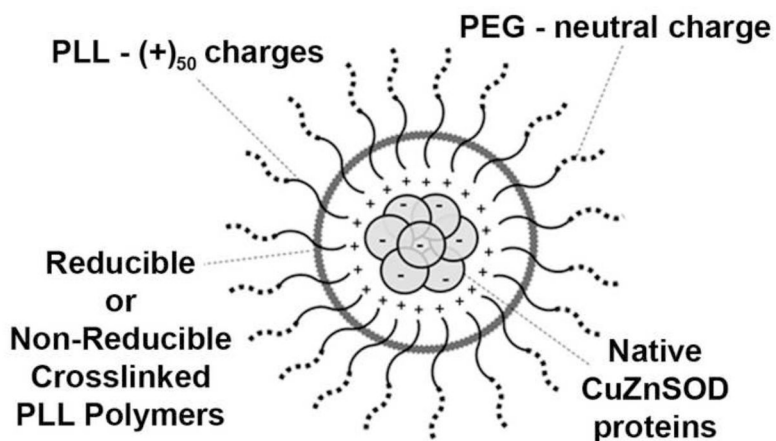


**FIGURE 1. Schematic of PLL<sub>50</sub>-PEG CuZnSOD Nanozyme**

Block copolymer of poly-L-lysine (PLL<sub>50</sub>)-polyethylene glycol (PEG) electrostatically binds to native CuZnSOD protein. Two distinct formulations of the nanozyme have been synthesized with reducible or non-reducible crosslinked bonds between PLL polymers to create covalently stabilized complexes.



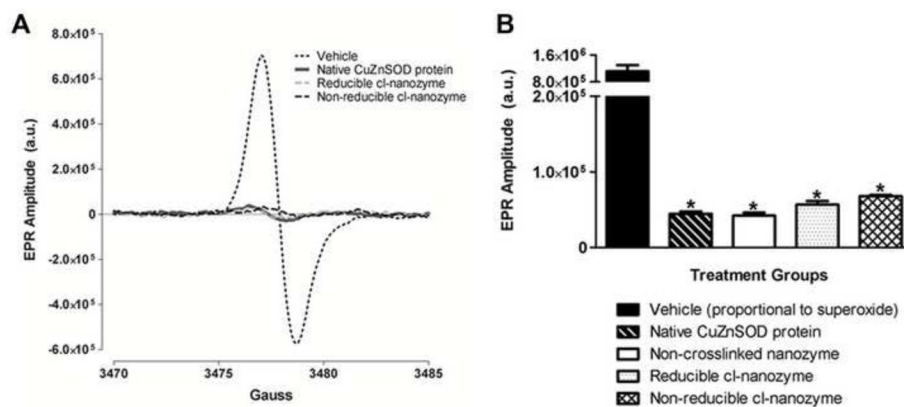


### FIGURE 2. CuZnSOD nanozymes scavenge superoxide

(A) Representative EPR spectra of the  $O_2^{\bullet-}$  sensitive CMH spin probe in cell-free samples treated with vehicle, native CuZnSOD protein, reducible cl-nanozyme, or non-reducible cl-nanozyme. Superoxide was generated in these cell-free samples by hypoxanthine and xanthine oxidase. (a.u. – arbitrary units). (B) Summary EPR spectroscopy data showing CMH spectra amplitude, which is directly proportional to the amount of  $O_2^{\bullet-}$  in the sample, in hypoxanthine/xanthine oxidase-containing samples treated with vehicle, native CuZnSOD protein, non-crosslinked nanozyme, reducible cl-nanozyme, or non-reducible cl-nanozyme ( $n = 4-5$  per group). Data represent mean  $\pm$  SEM. \*  $P < 0.05$  vs. vehicle.

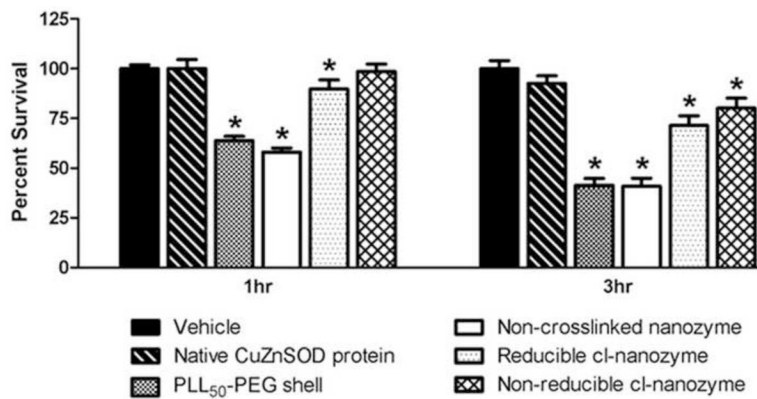


**FIGURE 3. Non-reducible cl-nanozyme is the least toxic nanozyme formulation**

Summary data showing CATH.a neuronal survival 24 hours after neurons were treated with vehicle, native CuZnSOD protein, PLL<sub>50</sub>-PEG shell, non-crosslinked nanozyme, reducible cl-nanozyme, or non-reducible cl-nanozyme for 1 or 3 hours (400U/mL of CuZnSOD was used for all CuZnSOD treatments). n = 4 separate neuronal cultures for native CuZnSOD protein; n = 10 separate neuronal cultures for all other groups. Data represent mean ± SEM. \* *P* < 0.05 vs. vehicle.

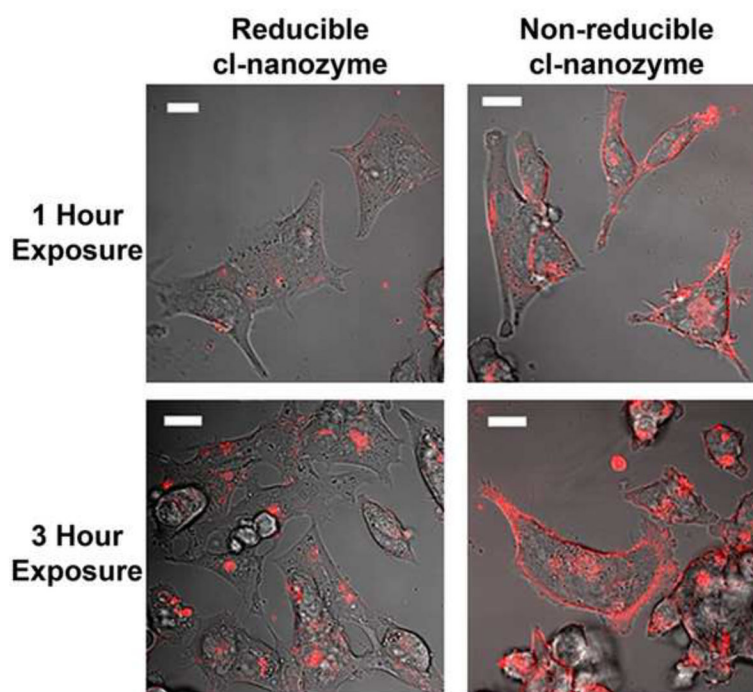


**FIGURE 4. Neuronal uptake of CuZnSOD crosslinked nanozymes**  
Representative confocal microscopy images from three independent experiments of CATH.a neurons exposed to rhodamine-labeled reducible or non-reducible cl-nanozyme (400U/mL of CuZnSOD) for 1 or 3 hours. Magnification bar = 20μm.

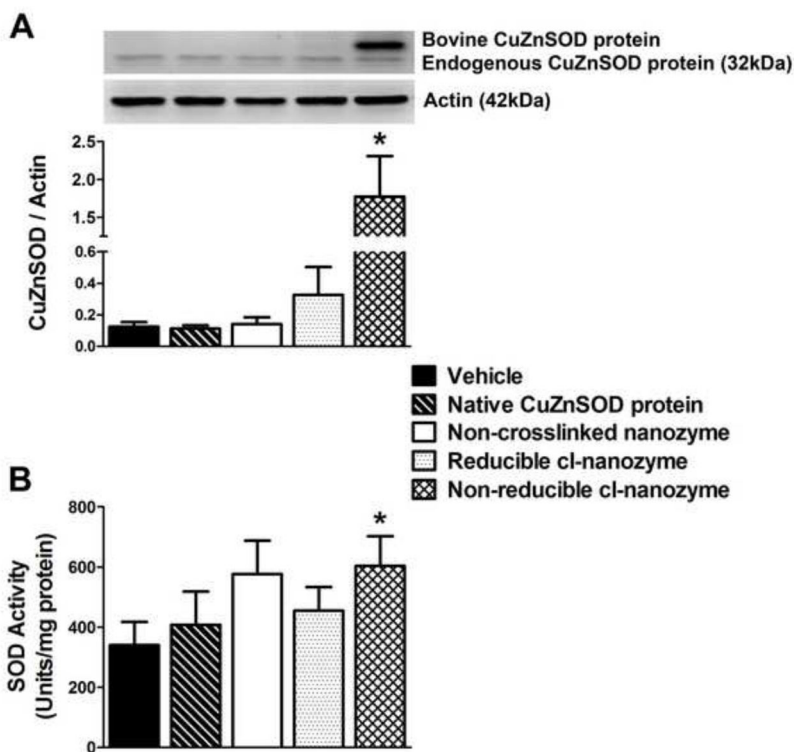


**FIGURE 5. Non-reducible cl-nanozyme delivers active CuZnSOD protein most efficiently to neurons in culture**

(A) Representative Western blot and summary quantification from lysates of CATH.a neurons treated (3 hours) with vehicle, native CuZnSOD protein, non-crosslinked nanozyme, reducible cl-nanozyme, or non-reducible cl-nanozyme (400U/mL of CuZnSOD was used for all CuZnSOD treatments). \* $P < 0.05$  vs. vehicle. (B) Summary data showing SOD activity in CATH.a neurons incubated for 3 hours with the same treatments listed above (A).  $n = 4-5$  separate neuronal cultures per group. Data represent mean  $\pm$  SEM. \*  $P < 0.05$  vs. vehicle.

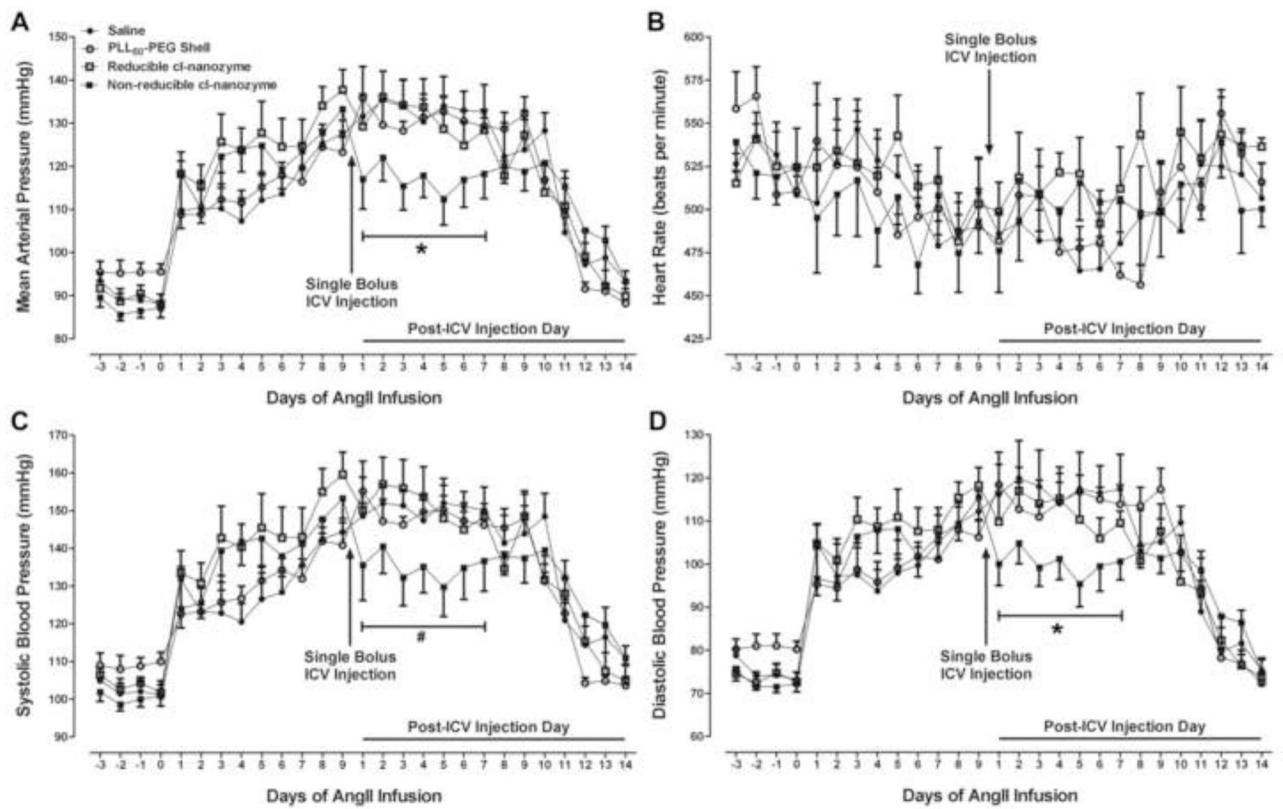


**FIGURE 6. ICV-administered non-reducible cl-nanozyme decreases blood pressure in AngII-dependent hypertensive mice**

Mean data showing AngII-induced changes in mean arterial pressure (A), heart rate (B), systolic blood pressure (C) and diastolic blood pressure (D) following subcutaneous infusion of AngII (400ng/kg/min) and changes in these physiological parameters after a single bolus ICV injection of saline, PLL<sub>50</sub>-PEG shell, reducible cl-nanozyme, or non-reducible cl-nanozyme (130–150 U of CuZnSOD was used for nanozyme treatments).  $n = 5-7$  mice per group. Data represent mean  $\pm$  SEM. \*  $P < 0.05$  vs. ICV-injected saline; #  $P = 0.085$  vs. ICV-injected saline.